Acta Geodyn. Geomater., Vol. 22, No. 4 (220), 571–584, 2025
DOI: 10.13168/AGG.2025.0041
journal homepage: https://www.irsm.cas.cz/acta

ORIGINAL PAPER

CAN SATELLITE GRAVINETRY DETECT SEDIMENT ACCUMULATIONS IN THE EAST CHINA SEA?

Meiqian GUAN [1] *, Zhiqiang LIAN [1] and Dapeng MU [2]

[1] *Weihai Vocational College, Weihai 264210, China*
[2] *Institute of Space Sciences, Shandong University, Weihai 264209, China*

**Corresponding author's e-mail:* guanmq0903@126.com

ARTICLE INFO

Article history:
Received 10 June 2025
Accepted 25 November 2025
Available online 15 December 2025

Keywords:
Time variable gravity
Sea level change
Coastal sediment

ABSTRACT

Several studies suggested that the Gravity Recovery and Climate Experiment (GRACE) satellite mission was capable of detecting sediment accumulation (about 6 mm/yr or 0.8 Gt/yr) in the East China Sea (ECS). Here we revisit this topic by evaluating GRACE observations for 2003-2015, in conjunction with satellite altimetry and Argo floats. Our investigation highlights the nature of geophysical signals observed by GRACE, and the process of leakage correction. Our analysis suggests that seasonal variations in the ECS are primarily induced by the combination of steric effect and water mass changes, which is demonstrated by the consistency between GRACE, satellite altimetry, and Argo. After applying the leakage correction, we show that the GRACE trend agrees with the steric-corrected altimeter trend, within the estimated uncertainty, indicating that the mass increase observed by GRACE should be mainly attributed to water instead of sediment. This conclusion is supported by a simulation based on in situ measurements of sediments. Our results suggest that sediment accumulation cannot be robustly separated from GRACE.

1. INTRODUCTION

The present study concerns the detection of sediment accumulation in the East China Sea (ECS) by a space geodesy technique, i.e., the Gravity Recovery and Climate Experiment (GRACE) mission (Tapley et al., 2019), which started mapping global time-variable gravity field since 2002. Time-variable gravity is tightly linked to global water-mass transport (Wahr et al., 1998; Wu et al., 2010; Croteau et al., 2020; Wang et al., 2025), mainly including water storage variations (Feng et al., 2018; Zhong et al., 2018; Scanlon et al., 2019; Jensen et al., 2019), and ocean mass changes (Chambers et al., 2004; Cazenave et al., 2009; Yi et al., 2015; Makowski et al., 2015; Kusche et al., 2016; Chen et al., 2018; Mu et al., 2020; Bonin and Save, 2020). In theory, sediment accumulation is detectable with GRACE, provided that its signal magnitude is larger than GRACE uncertainty. Some recent studies claimed that GRACE observations can reflect sediment accumulations in the ECS (e.g., Liu et al., 2016; Chang et al., 2019).

The ECS was indeed experiencing sediment accumulation across various time scales (Xu et al., 2009; Qiao et al., 2017), from days to thousands of years. For instance, sediment core measurements had indicated that sediment accumulation occurred along the coast of the ECS (e.g., Qiao et al., 2017), especially at the estuary of Yangtze River. In addition, a model study suggested that sediment from Yangtze River was mainly transported to the mud patch of the coast of the ECS (e.g., Bian et al., 2013; Fig. 1), and part of this sediment was carried to the Yellow Sea Trough. This finding was in contrast to some traditional views, e.g., Liu et al. (2007), and Yuan et al. (2008), who argued that the Taiwan Warm Current blocked the sediment, which was then deposited. While both model results and observations demonstrated sediment accumulation in the ECS, which causes gravity changes, the question is whether or not it can be detected by GRACE.

Recent studies suggested that GRACE had the ability to observe sediment accumulation in the ECS. Liu et al. (2016) derived a 6 mm/yr sediment mass rate using GRACE spherical harmonic coefficients (SHCs) product that had been corrected for the leakage from land water mass into oceans. By analyzing GRACE observations in conjunction with satellite altimetry and other data sources, Chang et al. (2019) reported strong seasonal variations of sediment changes in the ECS. Note that both Liu et al. (2016) and Chang et al. (2019) considered the leakage issue in GRACE, which was shown to be more serious along coastal zone (e.g., Baur et al., 2009; Tang et al., 2012; Mu et al., 2020). In the spatial pattern of global mass variations delivered by GRACE, the strong signals from land areas (e.g., ice mass loss, and land hydrology) tend to spread into oceans, this phenomenon is termed "leakage". The leakage influence on ocean signal is

Cite this article as: Guan M, Lian Z, Mu D: Can satellite gravimetry detect sediment accumulations in the East China Sea? Acta Geodyn. Geomater., 22, No. 4 (220), 571–584, 2025. DOI: 10.13168/AGG.2025.0041

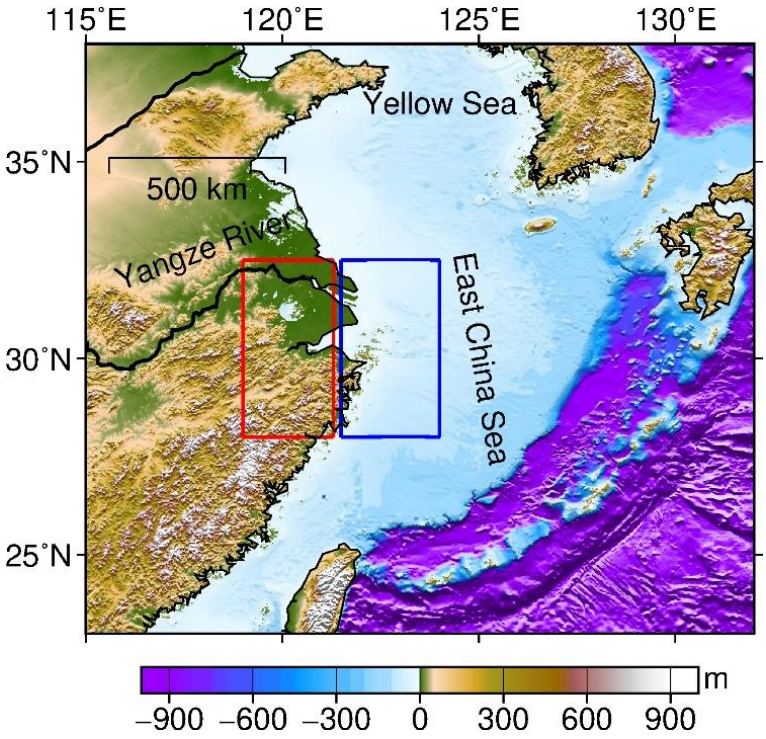

Fig. 1 Map of the East China Sea (ECS). Our ECS region is define as the blue box (approximately 240 km × 500 km). The nearby red box over land area is used to evaluate the leakage effect.

particularly strong over coastal zone. Given that sediment accumulations commonly occur along coasts, it is important to evaluate the leakage along a narrow coastal zone, such as the region defined by this paper (see the blue box in Figure 1).

In addition, to attribute the signals observed by GRACE, it is necessary to fully recognize their nature. Over the oceans, GRACE detects changes in ocean bottom pressure (including ocean mass variations and atmospheric mass variations), and other mass variation processes, e.g., possible sediment accumulations. The GRACE community routinely pre-remove some modeled signals from the GRACE products. These signals are simulated by geophysical models, including ocean models and atmosphere models (Flechtner et al., 2014), reflecting changes in ocean bottom pressure, which are called "GAD". The residual after the removal of GAD is called "GSM", which contains signals that are not modelled by the GAD, for example, some residual ocean mass variations at regional scale and their global mean, and sediment accumulation if it occurs (and is detectable by GRACE). We emphasize that the GAD filed is free of the striped noise, as it represents physical simulations; on the other hand, the GSM filed is filled with the striped noise that should be reduced by filtering techniques. We therefore must process the GAD and GSM differently regarding the noise reduction. Specifically, the filtering techniques can only be applied to the GSM field.

In this paper, we revisit the detection of sediment accumulation in the ECS, using GRACE data, along with altimeter measurements and steric component from Argo floats. We individually examine the GSM and GAD products, and highlight the comparisons of temporal changes between the GRACE estimates and steric-corrected altimeter measurements.

2. DATA

2.1. GRACE DATA

To estimate regional gravity changes, we use GRACE RL06 data covering the period 2003-2015. Two types of Center for Space Research (CSR) RL06 data are considered. The first one is the classic SHCs. The second type is the gridded product, i.e., mascon solutions (Save et al., 2016; Watkins et al., 2015). Given that there are several missing months in GRACE time series, we use cubic spline interpolation to get complete time series, which is more comparable to other time series, e.g., sea level time series from altimeter measurements.

To estimate gravity changes in the ECS, GRACE SHCs released by CSR, are processed in following steps. We first remove from the GSM product the background value that is estimated to be the mean value of the GSM over 2003 to 2015; we augment the GSM product with geocenter variations that are modelled by Sun et al. (2016), and replace the original GRACE C_{20} with those resolved by the satellite laser ranging (SLR; Loomis et al., 2019). Following the recommendation by Loomis et al. (2020), the original GRACE C_{30} is substituted with the SLR solutions for 2012-2015. The resulting GSM field is then corrected for the Glacial Isostatic Adjustment (GIA) effect using

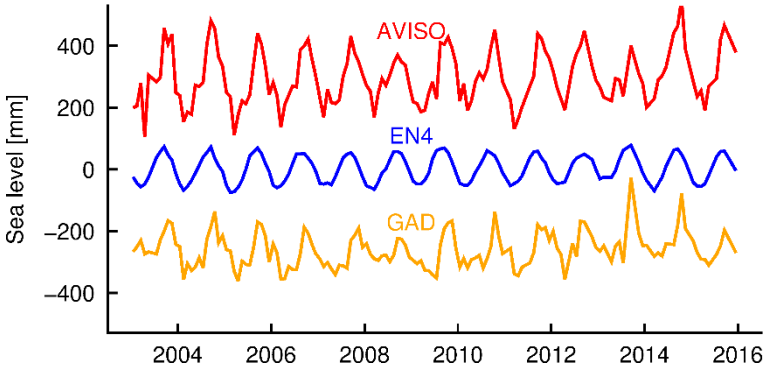

Fig. 2 The sea level changes over the East China Sea (ECS; blue box defined in Figure 1) from various data sources. Note that no filter is applied to these data. Vertical offsets are applied for viewing clarity.

the model of ICE-6G_D (Peltier et al., 2018). The reprocessed GSM field is finally converted to equivalent water heights (EWHs) with 300 km Gaussian filter (e.g., Wahr et al., 1998; Guo et al., 2014; Yan et al., 2016). Those EWHs should be further corrected for the leakage effect, this issue will be addressed in section 3.

As mentioned in introduction, the GSM field contains only residual signals. To fully evaluate the gravity changes in the ECS, we should add the GAD signal back into GRACE estimates. In this paper, we independently compute EWHs from the GAD product, without applying the filter technique. Given that the GAD field represents changes in ocean bottom pressure rather than ocean mass variations, we remove the global mean value of the GAD to obtain regional ocean mass changes (e.g., Uebbing et al., 2019).

Also used is the CSR RL06 mascon solutions (CSRM), which was resolved with regularization technique (Save et al., 2016). The mascon solutions represent global surface mass transport, and can be directly used without any post-processing. Note that, over the oceans, the mascon solutions describe changes in ocean bottom pressure instead of ocean mass variations. To derive ocean mass variations from the CSRM, we also remove the global mean of the GAD, consistent with the data-processing for the SHCs. The finally released mascon solutions are gridded into a 0.25-degree regular grid, but this grid does not reflect the real spatial resolution of GRACE.

2.2. ALTIMETER MEASUREMENTS

To interpret the gravity changes in the ECS, sea level anomalies (SLAs) measured by altimeters are used. These SLAs, produced by SSALTO/DUACS (Segment Sol multimissions d'ALTimétrie, d'Orbitographie et de localisation precise/Data Unification and Altimeter Combination System), and distributed by Archiving Validation and Interpretation of Satellite Oceanographic (AVISO, 2018), are gridded into a 0.25° regular grid at monthly intervals. Figure 2 shows the mean SLAs time series for the ECS that are averaged in the blue box defined in Figure 1. We clarify that the SLAs are directly averaged from original grid, and not processed with filtering technique. It is evidently observed that sea level changes in the ECS are primarily dominated by seasonal cycles (Fig. 2), which may be caused by ocean mass variations, steric components, and possibly the sediment accumulation. The GIA correction is applied to the SLAs using the ICE-6G_D model.

2.3. OCEAN ANALYSIS

To estimate steric sea level changes in the ECS, we use an ocean analysis provided by Met Office Hadley Centre (Good et al., 2013). This dataset is called EN4.2.1 (or EN4 for short); it assimilates various in-situ observations, including those from Argo floats (see Good et al., 2013 for more information). EN4 is generated with an objective analysis of global quality-controlled ocean temperature and salinity profiles. The EN4 data have a 1° horizontal resolution and 42 uneven vertical levels (down to 5000 m) of ocean temperature and salinity. More importantly, the EN4 covers most of global oceans, including coastal zones such like the ECS. The steric component estimated from EN4 suggests apparent annual cycles for the ECS (Fig. 2).

2.4. HYDROLOGY MODEL

To quantify the leakage from land areas into oceans, land water mass variations are required. Here we consider soil moisture storage estimated by the Global Land Data Assimilation System (GLDAS) Noah Version 2.1 (Rodell et al., 2004). This land surface model was developed by the National Aeronautics and Space Administration and the National Oceanic and Atmospheric Administration, it was constrained by both ground- and space-based observations. The GLDAS model provides users with optimally simulated fields of land surface states and fluxes, including 4 layers of soil moisture down to 2m depth. We use the monthly GLDAS model with 1-degree spatial resolution over 2003-2015.

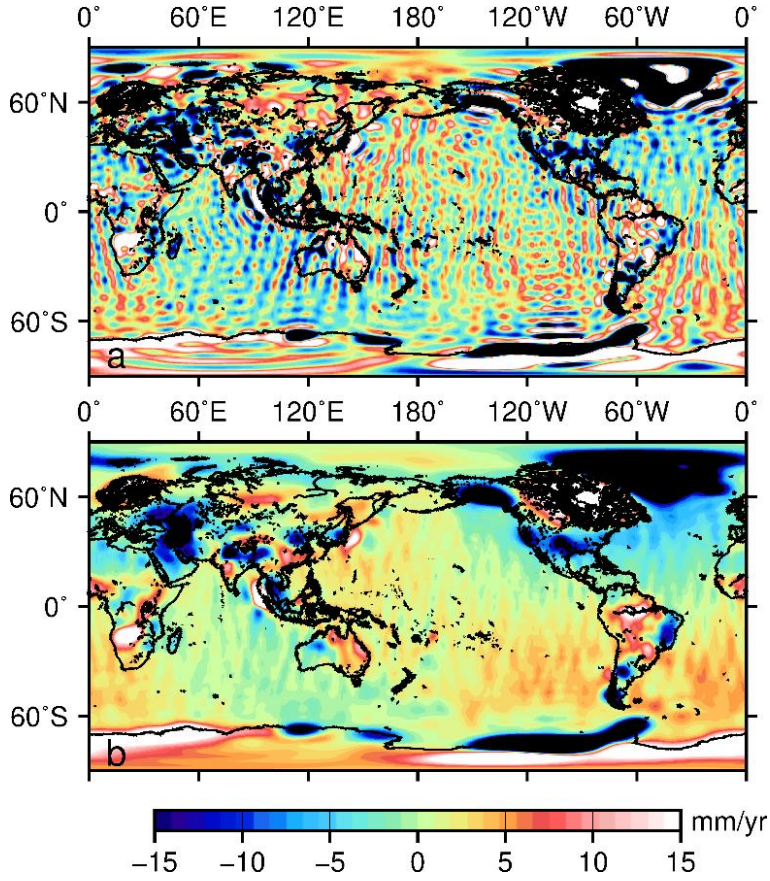

Fig. 3 GRACE GSM trends for the period 2003-2015. No filter is applied to (a), and (b) is filtered with 300 km Gaussian filter.

To obtain changes in land soil moisture, we first calculate the mean value for each grid point over the period 2003-2015, then remove the mean value from the monthly time series, the resulting anomalies represent land water mass variations. We emphasize that the GLDAS model serves to validate GRACE land mass variations near the coastline, because we must establish the dominant orientation for the leakage along the ECS (see more details in section 3).

3. CORRECTION OF GRACE LEAKAGE

We elaborate on a fundamental issue that concerns GRACE spatial variability, i.e., the leakage problem. In the early GRACE era, the GRACE SHCs were usually resolved at degree 60. Therefore, the half-wavelength of the maximum degree is estimated to be 330 km as follow:

$$\frac{0.5 \times Earth\ Circumference}{60} \approx 330\ km$$

The 300 km half-wavelength suggests that GRACE is only able to observe a regional mean change, instead of a point-referenced change. Specifically, the 'regional mean' implies that the mass variations from GRACE do not reflect in situ changes, but contain signals from surrounding areas, especially within several hundred kilometers. This characteristic is defined as leakage effect. By nature, the leakage effect represents the low spatial resolution of GRACE. The leakage effect becomes more complicated over coastal zone, because coastal mass variations include two disparate signals, one is from land, and another is from oceans. Mass variations usually show higher signal magnitudes over land areas than ocean mass variations. Consequently, land mass variations tend to leak into oceans, compromising ocean mass variations. However, in some cases, ocean signals are comparable to land signals (e.g., Mu et al., 2020), or even stronger, users should carefully interpret the leakage issue in GRACE mass variations.

There are apparent north-south stripes in the spatial pattern of EWH estimated from GRACE without filtering technique (Fig. 3a). Those stripes are time dependent and space specific (e.g., Yi et al., 2017), hampering the understanding of GRACE signals. To suppress the stripes, especially in high degree of SHCs, Gaussian filter (Jekeli, 1981) is widely applied. We stress that the Gaussian filter is only implemented for the GSM field, because the GAD field is simulated by geophysical models that are free of stripes. We smooth the GSM field with 300 km Gaussian filter (Fig. 3), which is found to be efficient over the ECS. The standard deviations of GSM are substantially reduced over the ECS after the

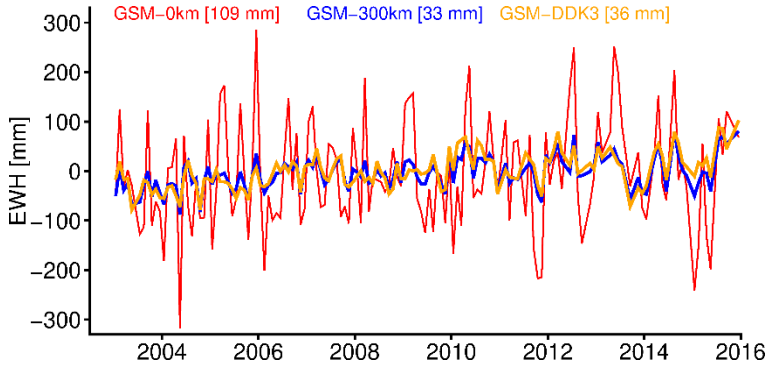

Fig. 4 Mass changes in the ECS (i.e., the blue box in Figure 1) from GRACE GSM with different filters; GSM-0 km (-300 km) represents Gaussian filter with 0 km (300 km), and DDK3 is a non-isotropic filter (see Kusche, 2007). The numbers in brackets indicate the standard deviations.

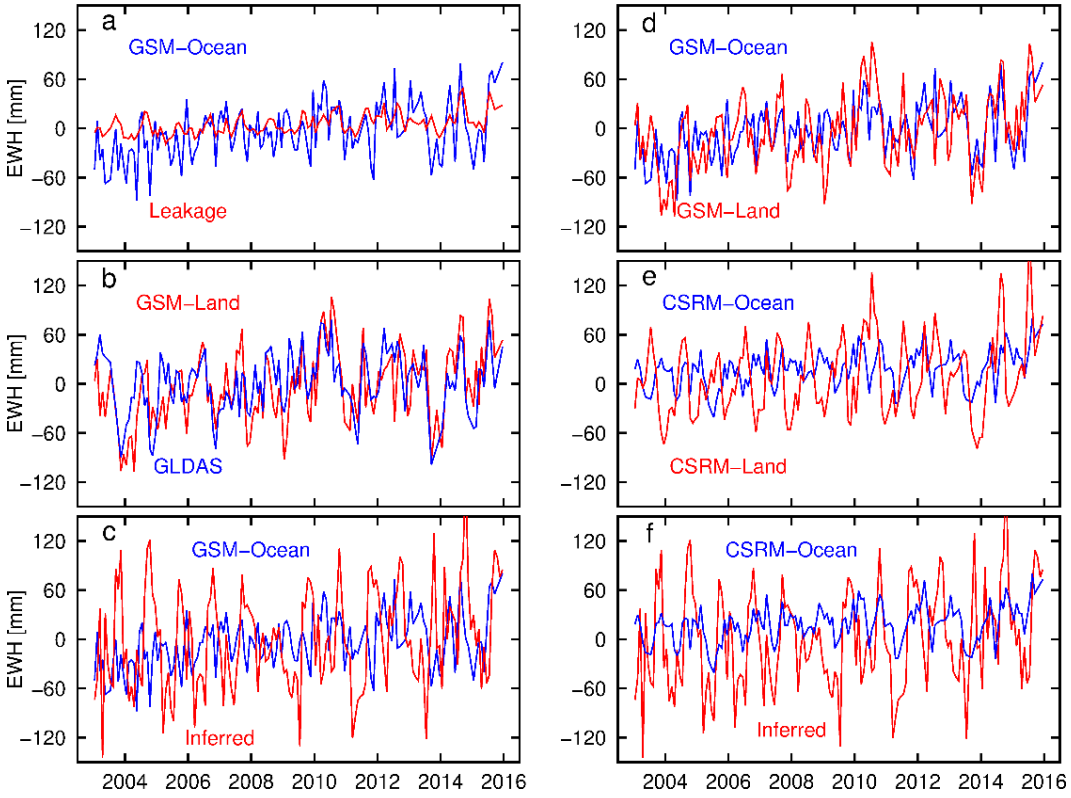

Fig. 5 Time series of mass changes in different box defined in Figure 1. (a) GSM-Ocean is computed with 300 km Gaussian filter, the leakage is simulated with CSR mascon (CSRM) land mass only (see text), these two series are averaged over the blue box (see Fig. 1); (b) GSM-Land is computed with 300 km Gaussian filter, and averaged over the red box (see Fig. 1); GLDAS is original output from the model, and averaged over the red box; (c) shows the comparison between GSM-Ocean (300km Gaussian filter) and the inferred time series, which is actually the difference between AVISO and EN4; (d) shows comparison between GSM-Ocean and GSM-Land, both are filtered with 300 km Gaussian filter, please note that GSM-Ocean has not been corrected for leakage; (e) shows comparison between CSRM-Ocean and CSRM-Land, and please note that CSRM-Ocean has the GAD components removed; (f) shows the comparison between the inferred results and CSRM-Ocean that has GAD removed.

implementation of 300 km Gaussian filter (see Fig. 4). To demonstrate that the Gaussian filter mainly reduces the noise, we compare GSM time series to GLDAS output over the region delineated by the red box (see Fig. 1) near the ECS. The comparison is shown in Figure 5b. We find a strong correlation (0.64±0.09) between GRACE and GLDAS, and their signal magnitudes are comparable (standard deviations are 41 mm and 38 mm, respectively) demonstrating that Gaussian filter efficiently reduces the noise.

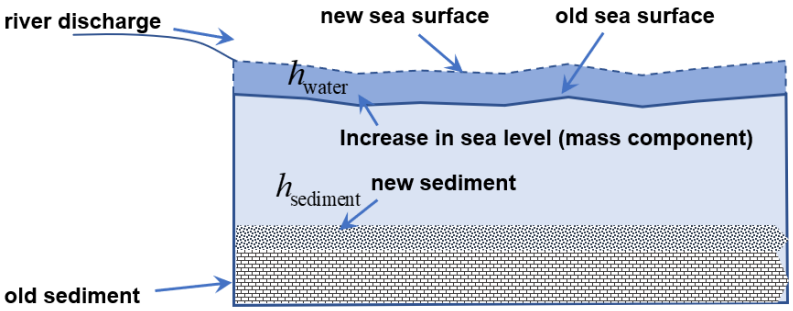

Fig. 6 Schematic relation between sediment and sea-water mass. The steric effect and GIA contribution are neglected here. The new sediment would replace sea-water, without affecting the local sea level; hence, the changes caused by $h_{sediment}$ is not observed by satellite altimetry, but can be detected by GRACE, the height estimated by GRACE is $\frac{\rho_s-\rho_w}{\rho_w}h_{sediment}$, ρ_s is the sediment density, and ρ_w is water density. Suppose the sea level has an increas h_{water} eowing to mass component, this increase can be detected by both satellite altimetry and GRACE. In conclusion, the GRACE observation $h_{GRACE}=\frac{\rho_s-\rho_w}{\rho_w}h_{sediment}+h_{water}$ should be larger than the altimetry observation $h_{altimetry}=h_{water}$, if there are any sediment depositions $h_{sediment}$.

However, the leakage issue is still required to be further addressed over the ECS. From Figure 5d, we find a visible correlation (0.42 ± 0.12) between land water mass signal (calculated from GSM with 300 km Gaussian filter, and averaged over the red box defined in Figure 1) and ocean mass variations in the ECS (i.e., the blue box defined in Figure 1), suggesting that land water mass leakage has an important effect on coastal ocean mass variations. We must carefully correct the leakage to obtain reliable signal for the ECS.

In theory, the leakage effect can be fully evaluated if the true mass variations over land areas are available. Unfortunately, this is unrealistic. We propose an alternative approach for approximately simulating the leakage. We assume that GRACE mascon is able to represent the "true" land water mass variations. We create a GRACE SHCs type signal by converting the CSRM land mass variations into SHCs. During this procedure, only land mass variations are considered, and ocean mass variations are masked out. We then compute EWHs from the resulting SHCs with 300 km Gaussian filter, those EWHs over the ECS represent the leakage from land water mass variations, and should be removed from the ocean mass variations that are calculated from original GRACE SHCs.

Using mascon solutions to simulate leakage is logical, because they have corrected the leakage along global coast (e.g., JPLM), or developed a dedicated method that prevents leakage from land into oceans (e.g., CSRM; Save et al., 2016). For example, mass variations from CSRM show distinct temporal fluctuations in red box and blue box (Fig. 5e), demonstrating a success of leakage correction. On the other hand, mass variations derived from GRACE SHCs appears to be correlated between the red box region (land area) and the blue box region (ocean area) (Fig. 5d).

4. INTERPRETATION OF GRACE MASS CHANGES

In this section, we interpret the mass variations from GRACE with the consideration of the leakage correction, and explore whether or not the GRACE detects the sediment accumulations over the ECS. We first formulate our basic logics. Figure 6 illustrates the schematic relation between the sediment accumulations and sea level changes. The new accumulations in sediment replace sea-water without altering the local sea surface. Since there are no geometrical changes in sea level, satellite altimetry does not observe any changes in sea level height, assuming zeros variations in steric effect. However, sediment accumulations induce changes in local gravity, because sediment density (ρ_s=1.6 g/cm^3) is larger than sea-water density (ρ_w=1.0 g/cm^3). A 1 mm sediment accumulation leads to increase in local gravity by $\frac{\rho_s-\rho_w}{\rho_w}$ mm, in terms of EWH. This quantitative relation suggests that GRACE EWH should be larger than the sea level heights retrieved from satellite altimetry with removal of the steric contributions, if the sediment accumulations are detectable by GRACE. We quantify this relation by using the following equation:

$$SL_{altimetry}-SL_{steric}=SL_{GSM}-SL_{leakage}+\\+SL_{GAD}+SL_{residual} \quad (1)$$

where the $SL_{altimetry}$ represents sea level changes from satellite altimetry, SL_{steric} is the steric contributions estimated from EN4, SL_{GSM} is the EWH estimated from GSM with 300 km Gaussian filter, $SL_{leakage}$ is the leakage correction, SL_{GAD} is the EWH estimated from GAD, $SL_{residual}$ is the residual EWH. The detection of sediment accumulations by GRACE

Table 1 Annual amplitude and linear rate for the ECS estimated from different datasets.

Data	Rate (mm/yr)	Amplitude (mm)	Phase (day)	RMS (mm)
AVISO	3.64±1.01	104±6	360	41
EN4	0.45±0.22	60±4	330	9
Leakage	0.68±0.16	12±8	290	8
GSM300	2.83±0.71	4±4	380	29
GAD	1.27±0.78	56±6	390	35
GF300	3.28±0.89	57±9	370	37
CSRM	4.03±0.87	66±8	370	36
Inferred	3.12±1.03	56±8	360	42

Note: Leakage is computed from CSR mascon (CSRM) land grids with 300 km Gaussian filter (see text for more details); GSM300 is computed from GSM field over the blue box (Fig. 1) with 300 km Gaussian filter, and it is corrected for GIA effect, but not the leakage listed here; GF300 represents the summation of "GAD + GSM300 – leakage"; the inferred results are defined as the difference between AVISO and EN4. Please notice that the rate and the annual amplitude are separately estimated from a robust least-squares method: we first fit linear rate, annual cycles, and semi-annual cycles to a robust regression, then the annual amplitude is derived; we then remove the fitted annual and semi-annual cycles, from the resulting residuals, we determine the linear trend via a robust regression again, to reduce the effect of seasonal changes on trend. All errors are standard errors produced by the robust regression.

would be demonstrated if $SL_{residual}$ is larger than the GRACE uncertainty. Note that equation 1 neglects the GIA effect, but it has been considered in our data processing. The difference between $SL_{altimetry}$ and SL_{steric} is termed 'inferred' ocean mass variations.

We briefly describe our strategy for estimating linear trends and annual amplitudes. First, a robust regression is applied to time series to determine trends, annual amplitudes, and semi-annual amplitudes. The annual amplitudes, along its phase, are then calculated, and illustrated in Table 1. We remove the fits from original time series, and the residuals are defined as non-seasonal fluctuations (see section 5), whose root mean square (RMS) are also shown in Table 1. To robustly estimate the linear trend, we remove the fitted annual cycles and semi-annual cycles, and then use again the robust regression to determine linear trends.

Figure 7 compares the inferred mass changes to different types of GRACE estimates. Notice that correlations are compute with removal of linear trends. The strong correlations and the comparable annual amplitudes (Table 1) suggest that seasonal changes observed by GRACE are mainly induced by water mass, instead of sediment accumulations. Moreover, it is shown that the GAD field captures the major changes in seasonal cycles. On the other hand, the GSM field mainly reflects non-seasonal fluctuations. Therefore, the combination of GSM and GAD does not significantly improve the correlation on seasonal scale. We find that the CSRM produces a stronger correlation (Fig. 7c), implying that mascon solutions yield improved water mass signals on seasonal scale. In addition to the strong correlations, we also identify amplitude consistency between the inferred EWH and GRACE EWH, especially, those from GRACE SHCs. The strong correlation and good consistency imply small or even negligible changes in $SL_{residual}$, demonstrating that GRACE estimates do not reflect seasonal sediment changes.

On seasonal scale, we exclude detectable sediment changes from GRACE over the ECS region. We now turn to the sediment accumulations by analyzing the linear trends. Table 1 illustrates the linear rate from different datasets over 2003-2015. The GF300 represents the combination of GAD and GSM field that is filtered with 300 km Gaussian filter, and corrected for the leakage, which shows a rate of 3.28±0.86 mm/yr. This rate is in excellent agreement with the inferred EWH rate (3.12±1.03 mm/yr). These two quantifications indicate that the mass changes from GRACE are mainly induced by water mass variations, because the GRACE rate would be larger than the inferred rate, if it contains significant sediment accumulations.

5. SEDIMENTATION SIMULATION

In this section, we perform a simulation to consolidate the conclusion from section 4. The simulation considers in situ sedimentary measurements collected by Qiao et al. (2017). Those measurements were sampled before 2000s (Fig. 8 and Table 2), reflecting point-referenced changes at sites in the ECS, and suggesting high spatial variability for sediment accumulations, especially along the coast.

The simulation is implemented as follow. First, we distribute the sediment accumulations over the region of blue box (Fig. 1). Qiao et al. (2017) derived a sediment rate of 0.56 Gt /yr for the ECS mud area (see Fig. 4 in Qiao et al., 2017). This mud area has a slightly longer North-South distance than our defined ECS. Given that we do not have sediment measurements for the period 2003-2015, we assume a rate of 0.56 Gt/yr over the GRACE era, although the sediment accumulation rate is expected to be reduced by anthropogenic changes (e.g., Qiao et al., 2017; Wang et al., 2016). Furthermore, we propose that these sediments are uniformly accumulated. Second, we transform the sediment accumulations into GRACE-

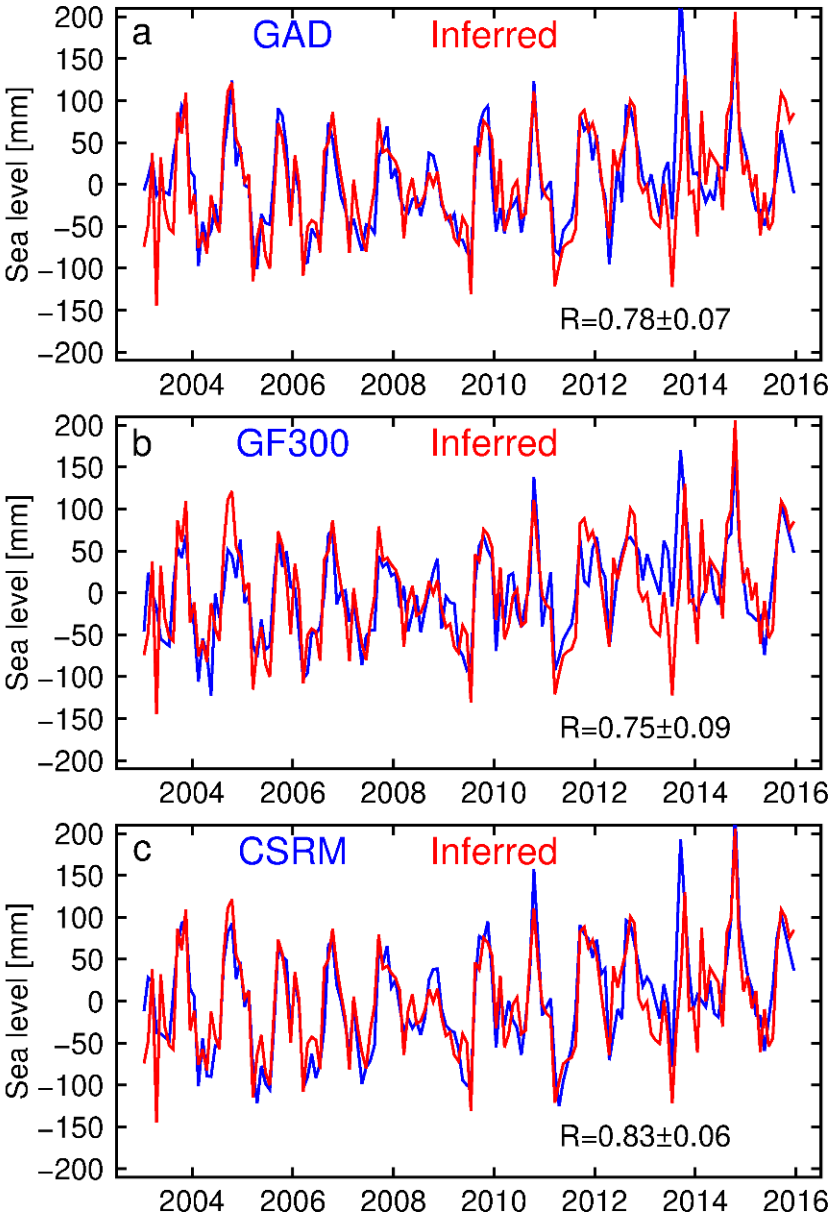

Fig. 7 Mass changes in the ECS. (a) shows comparison between GAD and the inferred results that are defined as "AVISO-minus-EN4"; (b) shows comparison between the inferred results and GF300, which represent the summation of GAD and GSM with 300 km filter (leakage is corrected for); (c) shows comparison between the inferred results and CSR mascon (CSRM). Black numbers indicate correlations that are computed from original time series, but with removal of linear trend.

type signal. By assuming a uniformly distributed pattern for the rate of 0.56 Gt/yr over the blue box (240 km × 500 km), we have the height for the increase of sediment: $\frac{0.56}{240\times500\times1.6}\times10^6 = 2.92$ mm/yr. The new sediments replace sea-water with the same volumes, hence, the resulting mass loss is $240\times500\times2.92\times10^{-6} = 0.35$ Gt/yr. The actual increase rate of local mass variations is 0.56 Gt/yr - 0.35 Gt/yr = 0.21 Gt/yr, which equals to $\frac{0.21}{240\times500\times1.0}\times10^6 = 1.75$ mm/yr in terms of EWH (Fig. 9a). This 1.75 mm/yr rate of EWH is converted into SHCs and are truncated at degree 60 (see Fig. 9b), which finally yields a 0.92 mm/yr rate of EWH.

This 0.92 mm/yr rate of EWH does not robustly demonstrate the detection of sediment accumulations by GRACE, because this rate falls within the uncertainty estimated for GRACE and the inferred mass variations (Table 1). Moreover, those uncertainty only represents formal error by least-squares fitting, and has not accounted for other uncertainty sources, e.g., uncertainty in GIA effect, uncertainty in steric sea level. Hence, those uncertainty very likely underestimates the uncertainty for the GRACE trends

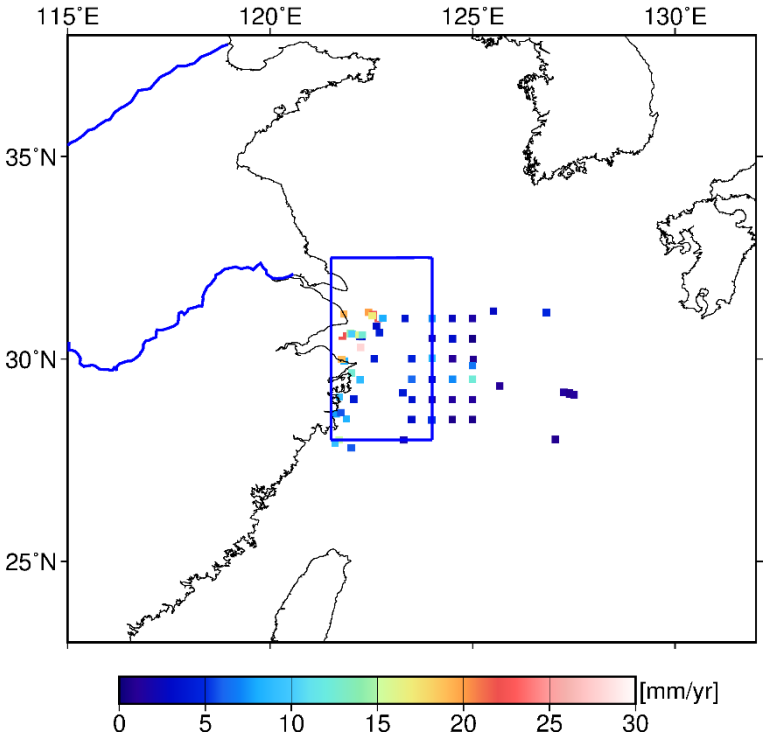

Fig. 8 The rate of sediment core measurements provided by Qiao et al. (2017).

Table 2 Rate of sedimentation estimated from different sediment measurements.

Longitude	Latitude	Rate (mm/yr)	Period	Data source
121.700056	28.000619	15	Pre-1998	Huh and Su, 1999
121.882491	28.525553	8.2	Pre-1998	Huh and Su, 1999
122.569308	30.000937	4.0	Pre-1998	Huh and Su, 1999
122.569308	30.319079	33	Pre-1998	Huh and Su, 1999
121.851282	31.298122	10.3	1995-2003	Wei et al.,2007
121.706406	31.260342	1.7	1995-2003	Wei et al.,2007
121.745000	28.675000	5.7	1990-1995	Xia et al., 1999
122.016667	29.648333	12.5	1990-1995	Xia et al., 1999
121.983074	30.630157	14.3	1991-1999	Xia et al.,2004
122.271401	30.548664	3.5	1991-1999	Xia et al.,2004

Note: these rates are shown in Figure 7, and provided by Qiao et al. (2017).

and the inferred trends. This issue is discussed in the next section.

6. DISCUSSION

6.1. UNCERTAINTY IN GRACE TREND ESTIMATES

The uncertainty associated with the trends of GRACE should be addressed. Our simulation suggests that the sediment accumulation rate that has been converted into GRACE-type signal has a similar magnitude to the trend uncertainty of GRACE estimates shown in Table 1. The uncertainty estimates only consider the formal error by least-squares fitting, and have not accommodated other uncertainty sources. Major uncertainty sources may originate from the corrections applied to the GRACE SHCs, including the GIA correction, the low-degree corrections, and the leakage correction.

Several studies have argued that the GIA correction for GRACE EWH suffers from an uncertainty up to about 0.4 mm/yr on global scale, even if the errors in ice history and Earth models are ignored (Tamisiea, 2011). We quantify the GIA correction difference between the ICE-6G_D model and the Aa et al. (2013) model and the Paulson et al. (2007) model over the ECS region. The comparison suggests a rate difference of 0.62 mm/yr between the ICE-6G_D and Aa et al. (2013), comparable to the signal of sediment accumulation simulated by this paper and the formal errors shown in Table1. The difference between the ICE-6G_D and Paulson et al. (2007) is reduce to 0.33 mm/yr over the ECS. Those comparisons confirm that the GIA correction is an important uncertainty source over the ECS region, impeding the conclusive detection of sediment accumulation by the GRACE observations.

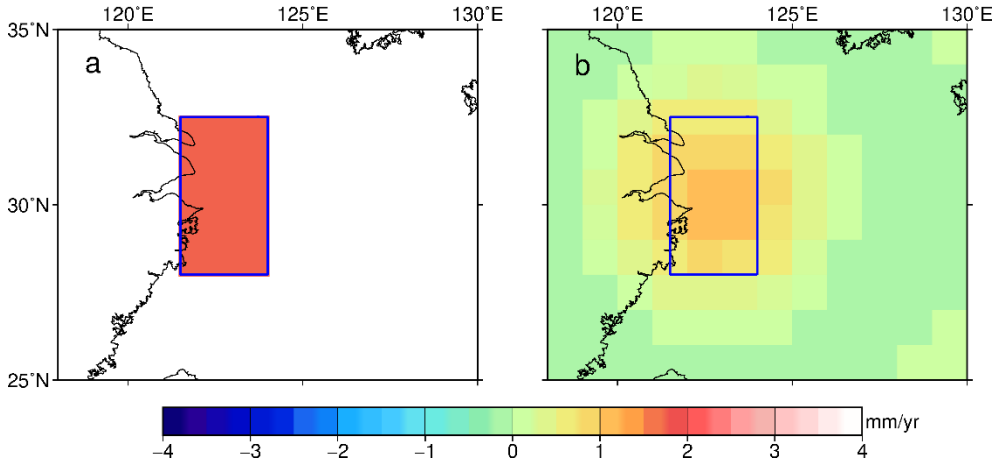

Fig. 9 Sedimentation simulation; (a) input sediment rate (1.7 mm/yr); the calculation of this input signal is described in section 5; (b) GRACE-like signal that is converted from (a) into spherical harmonic coefficients, and truncated at degree 60. Notice that we use the full blue box for simulation, to simplify the computation. Including small oceanic area causes only minor effect on our results.

In the GRACE data processing, it is a routine that the geocenter variations (i.e., degree-1 terms) are adopted from the estimates by Sun et al. (2016), and the C_{20} and C_{30} are replaced with the solutions by Loomis et al. (2019). However, these products introduce errors that are nonnegligible. For instance, the evaluation by Blazquez et al. (2018) suggests that the geocenter variations result in 0.21 mm/yr uncertainty over global oceans. We quantify this uncertainty in the ECS. To this end, we evaluate the difference between Sun et al. (2016) and the geocenter variations resolved with SLR by Cheng et al. (2010). Note that the former product is monthly solutions, but the latter has an interval with 60 days (bimonthly). Our evaluation shows that the rate difference is up to 0.75 mm/yr in the ECS region, although the SLR solutions are associated with larger uncertainty, this difference suggests that the geocenter variations are an important uncertainty source.

The leakage correction may contribute to the uncertainty of the GRACE trends. Our leakage correction relies on the CSRM, which is assumed to able to reflect true changes in land water mass. We further assess the leakage correction using the JPLM, and find a similar value (0.85 mm/yr). This correction is comparable to the correction of 0.68 mm/yr by the CSRM, demonstrating consistency between GRACE mascon solutions. However, our assumption may be challenged, as the GRACE may not properly represent water mass variations over a small region (e.g., the red box in Figure 1), and underestimate the mass variations owing to low spatial resolution. We stress that the nearby small region is particularly important for the assessment of leakage correction, because its contribution dominates the signal of leakage, especially if its mass variations are larger than the far-field (i.e., land areas outside the red box). Given that true water mass variations are not available (at least in the red box), we are impossible to assess the uncertainty in the leakage correction, but the difference between the CSRM and JPLM implies that it could be larger than 0.1 mm/yr.

In addition to the uncertainty sources considered above, the Gaussian filter may also attenuate the signal (e.g., the trend), and contribute to the trend uncertainty, despite the significant reduction of the stripes. We compare the Gaussian filter with the DDK3 filter (Kusche, 2007) for the GRACE trend (Fig. 10a), and find that the trend by the DDK3 filter is about 1.1 mm/yr larger than the trend by the Gaussian filter. This difference implies that the uncertainty by the Gaussian filter may be even comparable to the trend simulated with the in situ sediment measurements, challenging the ability of GRACE to sense the sediment accumulations.

6.2. NON-SEASONAL FLUCTUATIONS

Useful insights can be gained by examining non-seasonal fluctuations. Figure 11 shows non-seasonal fluctuations that are smoothed with 3-month moving average. Both GRACE SHCs and CSRM are well correlated with the inferred time series; the correlation between CSRM and the inferred variations is estimated to be 0.73±0.06, which is stronger than the correlation between SHCs and the inferred variations (0.60±0.08), suggesting improvements by the mascon solutions. In addition to correlations, excellent consistency in the signal magnitudes (i.e., standard deviations) is shown among the inferred mass variations, the CSRM, and GRACE SHCs (Fig. 11b), supporting that the non-seasonal fluctuations mainly reflect sea level changes, rather than sediment mass variations. It is also worth mentioning that steric contribution is secondary on non-seasonal scale (Fig. 11a); sea level non-seasonal changes in the ECS are mainly caused by ocean mass, suggesting the

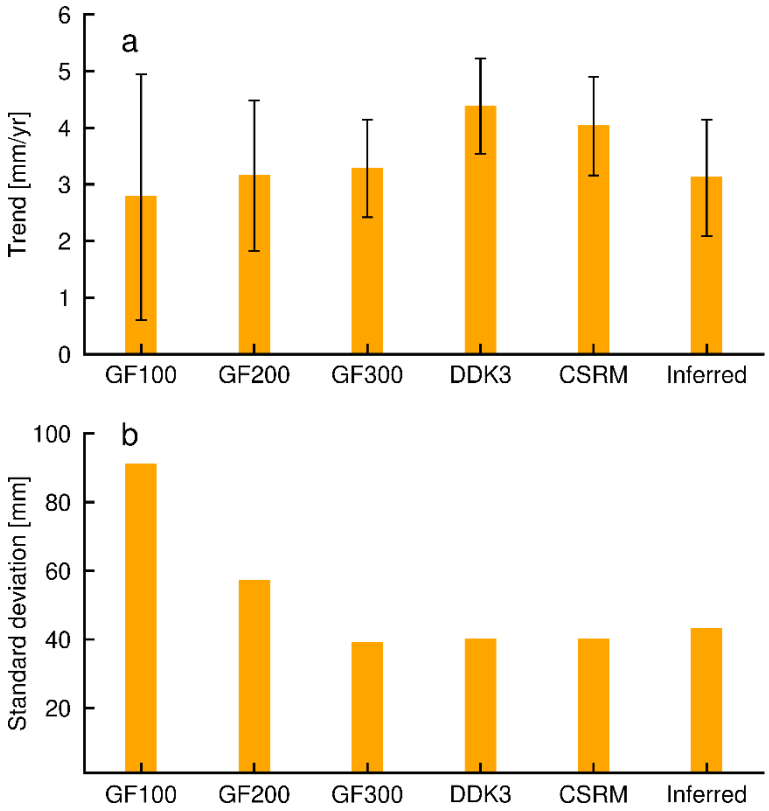

Fig. 10 Linear trend and variability of the ECS mass changes. (a) shows linear trends that are derived from different methods and sources, e.g., GF100 represents summation of GAD and GSM with 100 km Gaussian filter that is corrected for the leakage; DDK3 represents summation of GAD and GSM that is filtered with DDK3, but its leakage correction is computed with the 300 km Gaussian filter, because the explicit kernel of DDK3 is not available; please note the error bars are derived from a robust fitting at 1 σ; (b) shows the standard deviations of non-seasonal fluctuations of mass components. 'Inferred' is the inferred mass variations derived from the difference between satellite altimetry and the steric contributions.

dominant role of barotropic contribution. We highlight that our investigation focuses on the temporal variability, is different from the previous studies (e.g., Liu et al., 2016; Chang et al., 2019) with more emphasis on comparison of spatial variability.

7. CONCLUDING REMARKS

In this contribution, we reinvestigate the ability of GRACE to detect sediment accumulations in the ECS. Our results suggest that GRACE mass changes are mainly induced by water mass variations, instead of sediment mass changes, contradicting the conclusions by Chang et al. (2019) who derived sediment seasonal cycles, and by Liu et al. (2016) who concluded sediment accumulations from GRACE. We argue that temporal evolution of GRACE estimates (and its individual components) should be fully explored and assessed, especially for a narrow zone along coasts like the ECS.

ACKNOWLEDGMENTS, SAMPLES, AND DATA

This research was funded by the National Natural Science Foundation of China (Grant Nos. 42192534 and 42574001)

GRACE data is available from https://grace.jpl.nasa.gov, and CSR mascons can be downloaded from http://www2.csr.utexas.edu/grace/; AVISO data is downloaded at https://www.aviso.altimetry.fr.; EN4 data is available from https://www.metoffice.gov.uk/hadobs/en4/. The GLDAS data is available from https://ldas.gsfc.nasa.gov/gldas/.

Authors declare no financial conflicts of interests

REFERENCES

Aa, G., Wahr, J. and Zhong, S.: 2013, Computations of the viscoelastic response of a 3-D compressible Earth to surface loading: an application to Glacial Isostatic Adjustment in Antarctica and Canada. Geophys. J. Int., 192, 557–572. DOI: 10.1093/gji/ggs030

AVISO: 2018, SSALTO/DUACS user handbook: (M)SLA and (M)ADT near-real time and delayed time products CLS-DOS-NT-06-034, 4.1.

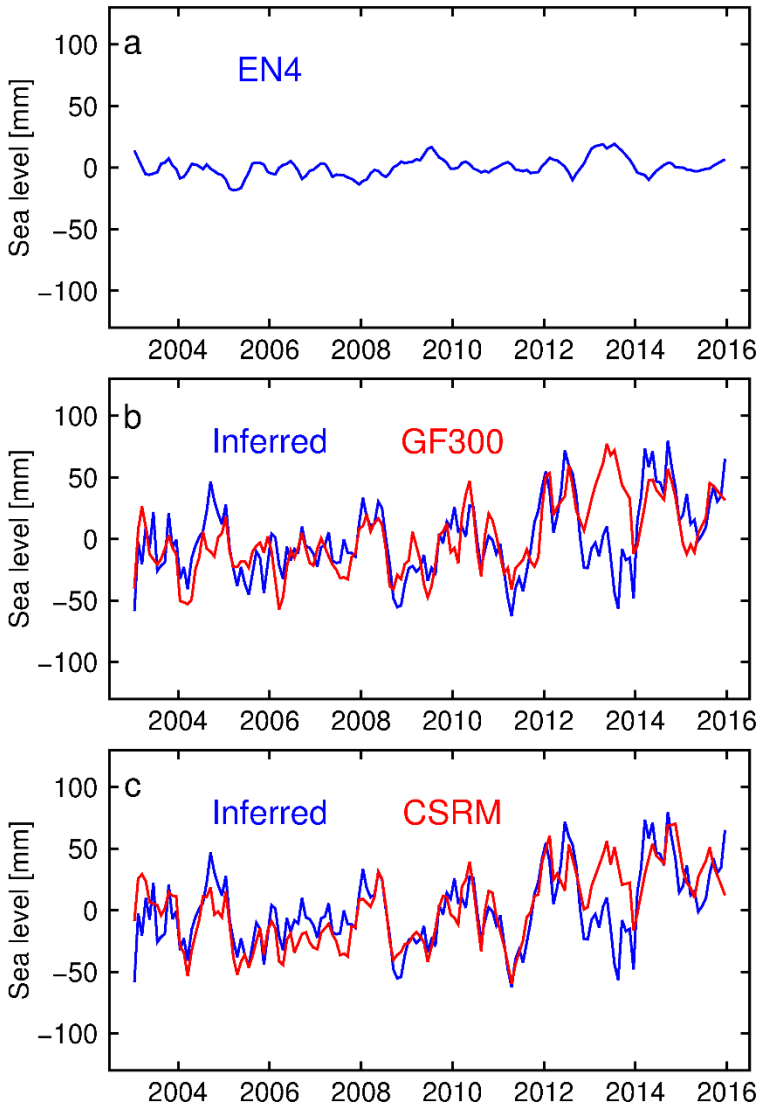

Fig. 11 Non-seasonal-fluctuations in the ECS; these fluctuations are computed from the time series shown in Figure 6. (a) Shows non-seasonal fluctuations for EN4; (b) shows comparison between the inferred results and GF300 (GF300 denotes the summation of GAD and GSM with 300 km Gaussian filter that is corrected for leakage); (c) compares the inferred mass variations with the CSR mascon (CSRM). The method used to compute non-seasonal fluctuations is described in section 4; note that a 3-month moving averaging is applied.

Baur, O., Kuhn, M. and Featherstone, W.E.: 2009, GRACE-derived ice-mass variations over Greenland by accounting for leakage effects. J. Geophys. Res., Solid Earth, 114. DOI: 10.1029/2008JB006239

Bian, C., Jiang, W. and Greatbatch, R.J.: 2013, An exploratory model study of sediment transport sources and deposits in the Bohai Sea, Yellow Sea, and East China Sea. J. Geophys. Res., Oceans, 118, 5908–5923. DOI: 10.1002/2013JC009116

Blazquez, A., Meyssignac, B., Lemoine, J.M., Berthier, E., Ribes, A. and Cazenave, A.: 2018, Exploring the uncertainty in GRACE estimates of the mass redistributions at the for the global water and sea level budgets. Geophys. J. Int., 215, 415–430. DOI: 10.1093/gji/ggy293

Bonin, J.A. and Save, H.: 2020, Evaluation of sub-monthly oceanographic signal in GRACE "daily" swath series using altimetry. Ocean Sci., 16, 423–434. DOI: 10.5194/os-16-423-2020

Cazenave, A., Dominh, K., Guinehut, S. et al.: 2009, Sea level budget over 2003-2008: A reevaluation from GRACE space gravimetry, satellite altimetry and Argo. Global Planet. Change, 65, 83–88. DOI: 10.1016/j.gloplacha.2008.10.004

Chambers, D.P., Wahr, J. and Nerem, R.S.: 2004, Preliminary observations of global ocean mass variations with GRACE. Geophys. Res. Lett., 31, L13310. DOI: 10.1029/2004GL020461

Chang, L., Tang, H., Yi, S. and Sun, W.: 2019, The trend and seasonal change of sediment in the East China Sea detected by GRACE. Geophys. Res. Lett., 46, 1250–1258. DOI: 10.1029/2018GL081652

Chen, J.L., Tapley, B., Save, H., Tamisiea, M.E., Bettadpur, S. and Ries, J.: 2018, Quantification of ocean mass change using Gravity Recovery and Climate Experiment, satellite altimeter, and Argo floats observations, J. Geophys. Res., Solid Earth, 123, 10,212–10,225. DOI: 10.1029/2018JB016095

Cheng, M.K., Tapley B.D. and Ries, J.C.: 2010, Geocenter variations from analysis of SLR data. IAG Commission 1, Symposium Reference Frames for Applications in Geosciences (REFAG2010), Marne-La-Vallee, France, 4-8 October 2010.

Croteau, M.J., Nerem, R.S., Loomis, B.D. and Sabaka, T.J.: 2020, Development of a daily GRACE mascon solution for terrestrial water storage. J. Geophys. Res., Solid Earth, 125, 3. DOI: 10.1029/2019JB018468

Feng, W., Shum, C.K., Zhong, M. and Pan, Y.: 2018, Groundwater storage changes in China from satellite gravity: An overview. Remote Sens., 10, 674. DOI: 10.3390/rs10050674

Flechtner, F., Dobslaw, H. and Fagiolini, E.: 2014, AOD1B product description document for product release 05, Rev. 4.2, May 20. Tech. Rep., GFZ German Research Centre for Geosciences, Potsdam.

Good, S.A., Martin, M.J. and Rayner, N.A.: 2013, EN4: Quality controlled ocean temperature. Geophys. Res., Oceans, 118, 6704–6716. DOI: 10.1002/2013JC009067

Guo, J., Mu, D., Liu, X., Yan, H. and Dai, H.: 2014, Equivalent water height extracted from GRACE gravity field model with robust independent component analysis. Acta Geophys., 62, 4, 953–972. DOI: 10.2478/s11600-014-0210-0

Jekeli, C.: 1981, Alternative methods to smooth the Earth's gravity field. Ohio State Univ., Columbus.

Jensen, L., Eicker, A., Dobslaw, H. and Stacke, T: 2019, Long-term wetting and drying trends in land water storage derived from GRACE and CMIP5 models. J. Geophys. Res., Atmospheres, 124, 9808–9823. DOI: 10.1029/2018JD029989

Kusche, J.: 2007, Approximate decorrelation and non-isotropic smoothing of time-variable GRACE-type gravity field models. J. Geod., 81, 733–749. DOI: 10.1007/s00190-007-0143-3

Kusche, J., Uebbing, B., Rietbroek, R., Shum, C.K. and Khan, Z.H.: 2016, Sea level budget in the Bay of Bengaal (2002-2014) from GRACE and altimetry. J. Geophys. Res., Oceans, 121, 1194–1217. DOI: 10.1002/2015JC011471

Liu, J., Xu, K., Li, A., Milliman, J.D., Velozzi, D.M., Xiao, S. and Yang, Z.: 2007, Flux and fate of Yangtze River sediment delivered to the East China Sea. Geomorphology, 85, 208–224. DOI: 10.1016/j.geomorph.2006.03.023

Liu, Y.-C., Hwang, C., Han, J., Kao, R., Wu, C.-R., Shih, H.-C. and Tangdamrongsub, N.: 2016, Sedimet-mass accumulation rate and variability in the East China Sea detected by GRACE. Remote Sens., 8, 777. DOI: 10.3390/rs8090777

Loomis, B.D., Rachline, K.E. and Luthcke, S.B.: 2019, Improved Earth oblateness rate reveals increased ice sheet losses and mass-driven sea level rise. Geophys. Res. Lett., 46, 6910–6917. DOI: 10.1029/2019GL082929

Loomis, B.D., Rachlin, K.E., Wiese, D.N., Landerer, F.W. and Luthcke, S.B.: 2020, Replacing GRACE/GRACE-FO C30 with satellite laser ranging; Impacts on Antarctic Ice Sheet mass change. Geophys. Res. Lett., 47, e2019GL085488. DOI: 10.1029/2019GL085488

Makowski, J. K., Chambers, D.P. and Bonin, J.A.: 2015, Using ocean bottom pressure from the gravity recovery and climate experiment (GRACE) to estimate transport variability in the southern Indian Ocean. J. Geophys. Res. Oceans, 120, 4245–4259. DOI: 10.1002/2014JC010575

Mu, D., Xu, T. and Xu, G.: 2020, An investigation of mass changes in the Bohai Sea observed by GRACE. J. Geod., 94, 79. DOI: 10.1007/s00190-020-01408-1

Paulson, A., Zhong, S. and Wahr, J.: 2007, Inference of mantle viscosity from GRACE and relative sea level data. Geophys. J. Int., 171, 497–508. DOI: 10.1111/j.1365-246X.2007.03556.x

Peltier, W.R., Argus, D.F. and Drummond, R.: 2018, Comment on "An assessment of the ICE-6G_C (VM5a) glacial isostatic adjustment model" by Purcell et al. J. Geophys. Res., Solid Earth, 123, 2019–2028. DOI: 10.1002/2016JB013844

Qiao, S., Shi, X., Wang, G., Zhou, L., Hu, B., Hu, L., Yang, G., Liu, Y., Yao, Z. and Liu, S.: 2017, Sediment accumulation and budget in the Bohai Sea, Yellow Sea and East China Sea. Mar. Geol., 390, 270–281. DOI: 10.1016/j.margeo.2017.06.004

Rodell, M. et al.: 2004, The global land data assimilation system. Bull. Am. Meteorol. Soc., 85, 381-394. DOI: 10.1175/BAMS-85-3-381

Save, H., Bettadpur, S. and Tapley, B.D.: 2016, High resolution CSR GRACE RL05 mascons. J. Geophys. Res., Solid Earth, 121, 7547–7569. DOI: 10.1002/2016JB013007

Scanlon, B.R., Zhang, Z., Save, H., Sun, A.Y., Müller, S.H., van Beek, L.P.H. et al.: 2018, Global models underestimate large decadal declining and rising water storage trends relative to GRACE satellite data. Proc. Natl. Acad. Sci. U. S. A., 115, 6, E1080–E1089. DOI: 10.1073/pnas.1704665115

Scanlon, B.R. et al.: 2019, Tracking seasonal fluctuations in land water storage using global models and GRACE satellites. Geophys. Res. Lett., 46, 5254–5264. DOI: 10.1029/2018GL081836

Sun Y., Riva R. and Ditmar P., 2016. Optimizing estimates of annual variations and trends in geocenter motion and J2 from a combination of GRACE data and geophysical models. J. Geophys. Res., Solid Earth, 121, 8352–8370. DOI: 10.1002/2016JB013073

Tamisiea, M.E., 2011. Ongoing glacial isostatic contributions to observations of sea level change. Geophys. J. Int., 186, 1036–1044. DOI: 10.1111/j.1365-246X.2011.05116.x

Tapley, B.D. et al.: 2019, Contributions of GRACE to understanding climate change. Nat. Clim. Change, 9, 358–369. DOI: 10.1038/s41558-019-0456-2

The IMBIE team: 2020, Mass balance of the Greenland ice sheet from 1992 to 2018. Nature, 579, 233–239. DOI: 10.1038/s41586-019-1855-2

Uebbing, B., Kusche, J., Rietbroek, R. and Landerer, F.W.: 2019, Processing choices affect ocean mass estimates from GRACE. J. Geophys. Res., Oceans, 124, 1029–1044. DOI: 10.1029/2018JC014341

Wahr, J., Molenaar, M. and Bryan, F.: 1998, Time variability of the Earth's gravity field: hydrological and oceanic effects and their possible detection using GRACE. J. Geophys. Res., 103, 30205–30229. DOI: 10.1029/98JB02844

Wang, S., Fu, B., Piao S., Lv Y., Ciais P., Feng X. and Wang Y.: 2015, Reduced sediment transport in the Yellow River due to anthropogenic changes. Nat. Geosc., 9, 38–41. DOI: 10.1038/ngeo2602

Wang, F., Geng, J., Shen, Y., Chen, J., Cazenave, A., Chen, Q., Chang, L. and Wang, W.: 2025, Sea level budget in the East China Sea inferred from satellite gravimetry, altimetry and steric datasets. Remote Sens., 17. DOI: 10.3390/rs17050881

Watkins, M.M., Wiese, D.N., Yuan, D.N. et al.: 2015, Improved methods for observing Earth's time variable mass distribution with GRACE using spherical cap mascons. J. Geophys. Res., Solid Earth, 120, 2649–2671. DOI: 10.1002/2014JB011547

Wu, X., Heflin, M.B., Schotman, H. et al.: 2010, Simultaneous estimation of global present-day water transport and glacial isostatic adjustment. Nat. Geosci., 3, 642–646. DOI: 10.1038/ngeo938

Xu, K., Milliman, J.D., Li, A., Liu, J.P., Kao, S.J. and Wan, S.: 2009, Yangtze- and Taiwan-derived sediments on the inner shelf of East China Sea. Cont. Shelf Res., 29, 2240–2256. DOI: 10.1016/j.csr.2009.08.017

Yan, H., Chen, W. and Yuan, L.: 2016, Crustal vertical deformation response to different spatial scale of GRACE and GCMs surface loading. Geophys. J. Int., 204, 505–516. DOI: 10.1093/gji/ggv385

Yi, S., Sun, W., Heki, K. et al.: 2015, An increase in the rate of global mean sea level rise since 2010. Geophys. Res. Lett., 42, 3998–4006. DOI: 10.1002/2015GL063902

Yi, S., Song, C., Wang, Q., Wang, L. and Heki, K: 2017, The potential of GRACE gravimetry to detect the heavy rainfall-induced impoundment of a small reservoir in the upper Yellow River. Water Resour. Res., 53, 6562–6578. DOI: 10.1002/2017WR020793

Yuan, D., Zhu, J., Li, C. and Hu, D.: 2008, Cross-shelf circulation in the Yellow and East China Seas indicated by MODIS satellite observations. J. Mar. Syst., 70, 137–149. DOI: 10.1016/j.jmarsys.2007.04.002

Zhong, Y., Zhong, M., Feng, W., Zhang, Z., Shen, Y. and Wu, D.: 2018, Groundwater depletion in the West Liaohe River basin, China and its implications revealed by GRACE and in situ measurements. Remote Sens., 10, 493. DOI: 10.3390/rs10040493